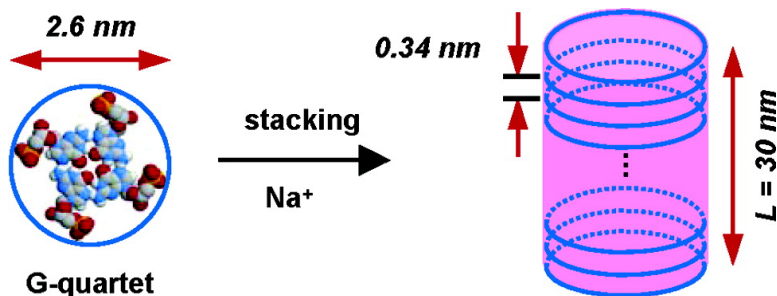


## Disodium Guanosine 5'-Monophosphate Self-Associates into Nanoscale Cylinders at pH 8: A Combined Diffusion NMR Spectroscopy and Dynamic Light Scattering Study

Alan Wong, Ramsey Ida, Lea Spindler, and Gang Wu

*J. Am. Chem. Soc.*, **2005**, 127 (19), 6990-6998 • DOI: 10.1021/ja042794d • Publication Date (Web): 21 April 2005

Downloaded from <http://pubs.acs.org> on March 25, 2009



### More About This Article

Additional resources and features associated with this article are available within the HTML version:

- Supporting Information
- Links to the 12 articles that cite this article, as of the time of this article download
- Access to high resolution figures
- Links to articles and content related to this article
- Copyright permission to reproduce figures and/or text from this article

[View the Full Text HTML](#)



## Disodium Guanosine 5'-Monophosphate Self-Associates into Nanoscale Cylinders at pH 8: A Combined Diffusion NMR Spectroscopy and Dynamic Light Scattering Study

Alan Wong,<sup>†</sup> Ramsey Ida,<sup>†</sup> Lea Spindler,<sup>‡</sup> and Gang Wu\*<sup>†</sup>

Contribution from the Department of Chemistry, Queen's University, 90 Queen's Crescent, Kingston, Ontario, Canada K7L 3N6, Faculty of Mechanical Engineering, University of Maribor, Smetanova 17, SI-2000 Maribor, Slovenia, and J. Stefan Institute, Jamova 39, SI-1000 Ljubljana, Slovenia

Received November 30, 2004; E-mail: gangwu@chem.queensu.ca

**Abstract:** We report a combined NMR and dynamic light scattering (DLS) study on the size of supramolecular structures formed by disodium guanosine 5'-monophosphate, Na<sub>2</sub>(5'-GMP), at pH 8. In general, two distinct types of aggregate species are present in an aqueous solution of Na<sub>2</sub>(5'-GMP). One type consists of stacking 5'-GMP monomers, and the other contains stacking G-quartets. Both types of aggregates can be modeled as rodlike cylinders. The cylinder diameter is 10 and 26 Å for monomer aggregates and quartet aggregates, respectively. For Na<sub>2</sub>(5'-GMP) concentrations between 18 and 34 wt %, the cylinders formed by stacking G-quartets have an average length between 8 and 30 nm, corresponding to a stack of ~24–87 G-quartets. These nanoscale aggregates are significantly larger than what had previously been believed for Na<sub>2</sub>(5'-GMP) self-association at pH 8. The length of both types of 5'-GMP aggregates was found to increase with Na<sub>2</sub>(5'-GMP) concentration but was insensitive to the added NaCl in solution. While the aggregate size for monomer aggregates increases with a decrease in temperature, the size of G-quartet aggregates is essentially independent of temperature. We found that the size of G-quartet aggregates is slightly larger in D<sub>2</sub>O than in H<sub>2</sub>O, whereas the size of monomer aggregates remains the same in D<sub>2</sub>O and in H<sub>2</sub>O. We observed a linear relationship between the axial ratio of the 5'-GMP cylinders and the Na<sub>2</sub>(5'-GMP) concentration for both types of 5'-GMP aggregates, which suggests a common stacking mechanism for monomers and G-quartets.

### Introduction

Guanosine 5'-monophosphate (5'-GMP) molecules can self-assemble into a highly ordered structure at neutral or slightly basic pH.<sup>1</sup> The basic building block of such a supramolecular structure consists of four guanine molecules held together by as many as eight Hoogsteen-type hydrogen bonds in a planar fashion. This structural motif is known as the G-quartet. The G-quartet is generally stabilized by monovalent cations such as Na<sup>+</sup>, K<sup>+</sup>, Tl<sup>+</sup>, and NH<sub>4</sub><sup>+</sup>. The most common mode of cation binding is the so-called sandwich mode where a cation is sandwiched between two G-quartets and coordinated to eight carbonyl O6 atoms. In the solid state, the disk-shaped G-quartets are stacked on top of one another with a twist of 30° between adjacent G-quartets, forming a continuous right-handed helix.<sup>2–4</sup>

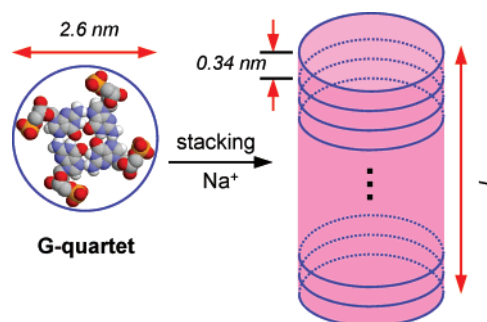


**Figure 1.** Schematic illustration of the molecular cylinder formed by Na<sub>2</sub>(5'-GMP) self-assembly.

The overall shape of this 5'-GMP supramolecular assembly can be modeled as a rodlike cylinder; see Figure 1. The interior of the cylinder is filled with monovalent cations such as Na<sup>+</sup> and K<sup>+</sup>.<sup>5–7</sup> Such a supramolecular structure is reminiscent of an ion channel. In solution, the same cylinder structure may also exist; however, the length of the cylinders must be finite. In the early NMR studies of Na<sub>2</sub>(5'-GMP) self-association, it was

<sup>†</sup> Queen's University.

<sup>‡</sup> University of Maribor and J. Stefan Institute.

- (1) For reviews on guanosine self-assembly, see: (a) Guschlbauer, W.; Chantot, J.-F.; Thiele, D. *J. Biomol. Struct. Dyn.* **1990**, *8*, 491–511. (b) Gottarelli, G.; Spada, G. P.; Garbesi, A. In *Comprehensive Supramolecular Chemistry*; Sauvage, J.-P., Hossenini, M. W., Eds.; Elsevier Science: Rugby, U.K., 1996; Vol. 9, pp 483–506. (c) Davis, J. T. *Angew. Chem., Int. Ed.* **2004**, *43*, 668–698.
- (2) Gellert, M.; Lipsitt, M. N.; Davies, D. R. *Proc. Natl. Acad. Sci. U.S.A.* **1962**, *48*, 2013–2018.
- (3) Zimmerman, S. B. *J. Mol. Biol.* **1976**, *106*, 663–672.
- (4) Lipanov, A. A.; Quintana, J.; Dickerson, R. E. *J. Biomol. Struct. Dyn.* **1990**, *3*, 483–489.

(5) Wu, G.; Wong, A. *Chem. Commun.* **2001**, 2658–2659.

(6) Wong, A.; Fetting, J. C.; Forman, S. L.; Davis, J. T.; Wu, G. *J. Am. Chem. Soc.* **2002**, *124*, 742–743.

(7) Wu, G.; Wong, A.; Gan, Z.; Davis, J. T. *J. Am. Chem. Soc.* **2003**, *125*, 7182–7183.

believed that the 5'-GMP aggregates are quite small at neutral or slightly basic pH, containing only octamers (2 G-quartet), dodecamers (3 G-quartets), or hexadecamers (4 G-quartets).<sup>8–18</sup> In 1992, Eimer and Dorfmueller<sup>19</sup> used depolarized dynamic light scattering (DDLS) and photon correlation spectroscopy (PCS) to determine the size of Na<sub>2</sub>(5'-GMP) self-aggregates at neutral pH. In aqueous solution, the hydrodynamic diameter of the 5'-GMP self-assembled cylinder is approximately 26 Å. On the basis of the measured rotational diffusion coefficients and a hydrodynamic theory, Eimer and Dorfmueller<sup>19</sup> concluded that, for Na<sub>2</sub>(5'-GMP) concentrations between 0.1 and 1.0 M, the average size of aggregates contains up to 18 stacks of G-quartets. These estimates are considerably larger than the size assumed in the earlier NMR studies.<sup>8–18</sup> Recently, Jurga-Novak et al.<sup>20</sup> applied PCS and depolarized Raleigh light scattering techniques to study 5'-GMP aggregation in both acidic and basic buffer solutions. They showed that, in an acidic buffer of pH 2, 5'-GMP aggregates can become large enough to contain a stack of 32 G-quartets, whereas in a slightly basic buffer of pH 7.3, the largest 5'-GMP aggregate contains only five G-quartets, much smaller than that determined by Eimer and Dorfmueller.<sup>19</sup> It should be noted that the 5'-GMP sample used in the study of Jurga-Novak et al.<sup>20</sup> was not a pure form of Na<sub>2</sub>(5'-GMP). In fact, the ratio between Na<sup>+</sup> ions and 5'-GMP molecules in their samples is less than 10%. This deficiency in Na<sup>+</sup> ions must be responsible for the observed discrepancy in 5'-GMP aggregate size between the two studies. In addition to solution acidity and cation concentration, the nature of the cation is also an important factor for 5'-GMP aggregation process. For example, Spindler et al.<sup>21,22</sup> showed that aggregates formed by the NH<sub>4</sub><sup>+</sup> salt of 2'-deoxyguanosine 5'-monophosphate, (NH<sub>4</sub>)<sub>2</sub>(5'-dGMP), contain more than a stack of 133 G-quartets at pH 5.6, which corresponds to a 45-nm-long molecular cylinder. Another example of guanosine-based self-assembly is the nanotubes (80–1500 nm) formed by calix[4]arene–guanosine conjugates, as reported by Davis and co-workers.<sup>23,24</sup>

Similar to 5'-GMP self-association, G-rich DNA oligomers can also form a variety of folded structures known as the G-quadruplex. NMR and crystallography are standard techniques

for obtaining detailed structural information for G-quadruplexes in solution and in the solid state, respectively. However, it is also often useful to obtain information about overall molecular shape and aggregate size without solving the entire G-quadruplex structure. For example, Gottarelli et al.<sup>25</sup> used small-angle X-ray scattering (SAXS) and small-angle neutron scattering (SANS) techniques to study the aggregate size for homoguanyl derivatives, d(G)<sub>m</sub> (m = 2–6). They showed that the length of the aggregates is less than 120 Å (36 G-quartets) under various salt and thermal conditions. Bolten et al.<sup>26</sup> used dynamic light scattering (DLS) techniques to examine the size and shape of three G-DNA oligomers: d(GGTTGGTGTGGTTGG), d(TTGGGGGTT), and d(TTGGGGTTGGGGTT). In the presence of NaCl or KCl, these DNA oligomers form either uni-, bi-, or tetramolecular G-quadruplex structures. No longitudinal stacking was found for these G-DNA oligomers. However, with a proper DNA sequence, longitudinal stacking is indeed possible. An extreme case for longitudinal stacking of G-DNA oligomers is the formation of nanoscale G-wires by a telomeric DNA repeat, d(GGGGTTGGGGG).<sup>27</sup> In the presence of Na<sup>+</sup> and Mg<sup>2+</sup>, the length of G-wires can be greater than 1000 nm, as imaged by atomic force microscopy (AFM).<sup>27</sup> Another possible way of forming higher aggregates is through an interlock mode as recently observed by Krishnan-Ghosh et al.<sup>28</sup>

In addition to the aforementioned DLS, SAXS, or SANS techniques, NMR spectroscopy is another powerful technique that can be used to obtain information about shape and size for molecular aggregates. Similar to DLS, diffusion NMR experiments can yield molecular translational diffusion coefficients for molecular aggregates, from which the geometrical size can be deduced.<sup>29</sup> For example, Davis and co-workers recently used diffusion NMR spectroscopy to characterize the self-association process of several guanosine nucleosides in organic solvents.<sup>30</sup> In the context of 5'-GMP self-association, Rymdén and Stilbs<sup>31</sup> published an article in 1985 where they used pulse-field-gradient (PFG) NMR techniques to measure translational diffusion coefficients for Na<sub>2</sub>(5'-GMP) at concentrations between 0.0344 and 0.363 M. However, at these concentrations, very few G-quartets (less than 1%) are present in solution at room temperature. Therefore, their NMR diffusion data reflect only equilibria involving 5'-GMP monomers. To the best of our knowledge, despite numerous NMR and DLS studies on Na<sub>2</sub>(5'-GMP) self-assembly, the aggregate size at neutral or slightly basic pH has not been unambiguously established. Here we use both diffusion NMR and DLS methods to determine the size of Na<sub>2</sub>(5'-GMP) aggregates at pH 8. We also examine the effects of concentration, temperature, solvent, and salt on the size of Na<sub>2</sub>(5'-GMP) aggregates.

- (8) Pinnavaia, T. J.; Miles, H. T.; Becker, E. D. *J. Am. Chem. Soc.* **1975**, *97*, 7198–7200.
- (9) Pinnavaia, T. J.; Marshall, C. L.; Mettler, C. M.; Fisk, C. L.; Miles, H. T.; Becker, E. D. *J. Am. Chem. Soc.* **1978**, *100*, 3625–3627.
- (10) Detellier, C.; Paris, A.; Laszlo, P. *C. R. Acad. Sci., Ser. D* **1978**, *286*, 781–783.
- (11) Delville, A.; Detellier, C.; Laszlo, P. *J. Magn. Reson.* **1979**, *34*, 301–315.
- (12) Borzo, M.; Detellier, C.; Laszlo, P.; Paris, A. *J. Am. Chem. Soc.* **1980**, *102*, 1124–1134.
- (13) Detellier, C.; Laszlo, P. *J. Am. Chem. Soc.* **1980**, *102*, 1135–1141.
- (14) Detellier, C.; Laszlo, P. *Helv. Chim. Acta* **1979**, *62*, 1559–1565.
- (15) Fisk, C. L.; Becker, E. D.; Miles, T. H.; Pinnavaia, T. J. *J. Am. Chem. Soc.* **1982**, *104*, 3307–3314.
- (16) Bouhoutsos-Brown, E.; Marshall, C. L.; Pinnavaia, T. J. *J. Am. Chem. Soc.* **1982**, *104*, 6576–6584.
- (17) Walmsley, J. A.; Barr, R. G.; Bouhoutsos-Brown, E.; Pinnavaia, T. J. *J. Phys. Chem.* **1984**, *88*, 2599–2605.
- (18) Walmsley, J. A.; Burnett, J. F. *Biochemistry* **1999**, *38*, 14063–14068.
- (19) Eimer, W.; Dorfmueller, Th. *J. Phys. Chem.* **1992**, *96*, 6790–6800.
- (20) Jurga-Novak, H.; Banachowicz, E.; Dobek, A.; Patkowski, A. *J. Phys. Chem. B* **2004**, *108*, 2744–2750.
- (21) Spindler, L.; Drevenšek-Olenik, I.; Čopič, M.; Romih, R.; Cerar, J.; Škerjanc, J.; Mariani, P. *Eur. Phys. J. E* **2002**, *7*, 95–102. Note that there is an error in this article. The length of the cylinder should be  $L = 450$  Å, corresponding to a stack of 133 G-quartets.
- (22) Spindler, L.; Drevenšek-Olenik, I.; Čopič, M.; Cerar, J.; Škerjanc, J.; Mariani, P. *Eur. Phys. J. E* **2004**, *13*, 27–33.
- (23) Sidorov, V.; Kotch, F. W.; El-Kouedi, M.; Davis, J. T. *Chem. Commun.* **2000**, 2369–2370.
- (24) Kotch, F. W.; Sidorov, V.; Lam, Y.-F.; Kayser, K. J.; Li, H.; Kaucher, M. S.; Davis, J. T. *J. Am. Chem. Soc.* **2003**, *125*, 15140–15150.

- (25) Gottarelli, G.; Spada, G. P.; Mariani, P. In *Crystallography of Supramolecular Compounds*; Tsoucaris, G., Atwood, J. L., Lipkowsky, J., Eds.; NATO Adv. Sci. Inst. Ser., Ser. C, Vol. 480; Kluwer Academic Publishers: Dordrecht, The Netherlands, 1996; pp 307–330.
- (26) Bolten, M.; Niermann, M.; Eimer, W. *Biochemistry* **1999**, *38*, 12416–12423.
- (27) (a) Marsh, T. C.; Henderson, E. *Biochemistry* **1994**, *33*, 10718–10724. (b) Marsh, T. C.; Vesenska, J.; Henderson, E. *Nucleic Acids Res.* **1995**, *23*, 696–700.
- (28) Krishnan-Ghosh, Y.; Liu, D.; Balasubramanian, S. *J. Am. Chem. Soc.* **2004**, *126*, 11009–11016.
- (29) Johnson, C. S., Jr. *Prog. Nucl. Magn. Reson. Spectrosc.* **1999**, *34*, 203–256.
- (30) Kaucher, M. S.; Lam, Y.-F.; Pieraccini, S.; Gottarelli, G.; Davis, J. T. *Chem.–Eur. J.* **2005**, *11*, 164–173.
- (31) Rymden, R.; Stilbs, P. *Biophys. Chem.* **1985**, *21*, 145–156.

## Experimental Section

**Sample Preparation.** Hydrated disodium salt of guanosine 5'-monophosphate,  $\text{Na}_2(5'\text{-GMP})\cdot x\text{H}_2\text{O}$ , was purchased from Sigma-Aldrich (Ontario, Canada). The purity of the compound is >99%.  $\text{Na}_2(5'\text{-GMP})$  samples were prepared in doubly distilled deionized water.

**NMR Experiments.** All  $^1\text{H}$  NMR spectra were recorded on Bruker Avance-500 and Avance-600 spectrometers. For  $^1\text{H}$  diffusion experiments, the pulse sequence of longitudinal eddy current delay (LED)<sup>32</sup> with bipolar-gradient pulses was used for samples in  $\text{D}_2\text{O}$  solvent. The  $^1\text{H}$   $90^\circ$  and  $180^\circ$  pulse widths were 10 and 20  $\mu\text{s}$ , respectively. The pulse field gradient duration ( $\delta$ ) was varied from 4 to 15 ms, and the variable gradient strength ( $G$ ) was changed from 6 to 350  $\text{mT}\cdot\text{m}^{-1}$ . The diffusion period ( $\Delta$ ) was varied from 50 to 90 ms. A total of 16 transients were collected for each of the 16 or 32 increment steps with a recycle delay of 10–20 s. The eddy current delay ( $t_e$ ) was set to 5  $\mu\text{s}$ . For samples using  $\text{H}_2\text{O}$  or a mixture of  $\text{D}_2\text{O}/\text{H}_2\text{O}$  as solvent, a WATERGATE sequence<sup>33</sup> was added into the LED sequence before data acquisition to achieve water suppression. For samples in pure  $\text{H}_2\text{O}$ , a small capillary tube filled with  $\text{D}_2\text{O}$  was placed inside the NMR tube to provide the  $^2\text{H}$  lock signal. All  $^1\text{H}$  NMR spectra were processed and analyzed with MestRe-C (Beta version 3.6.9). The sample temperature was carefully controlled with a Bruker BT-3000 unit. Calibration of the field gradient strength was achieved by measuring the value of translational diffusion coefficient ( $D_t$ ) for the residual  $^1\text{H}$  signal in  $\text{D}_2\text{O}$  (99.99%  $^2\text{H}$  atom),  $D_t = 1.90 \times 10^{-9} \text{ m}^2/\text{s}$ . The experimental diffusion data can be fitted into the following equation:<sup>34</sup>

$$I = I_0 \exp[-D_t \gamma_H^2 G^2 \delta^2 (\Delta - \delta/3)] \quad (1)$$

where  $I$  is the experimental signal intensity (or area),  $I_0$  is the initial signal intensity (or area), and  $\gamma_H$  is the magnetogyric ratio for  $^1\text{H}$ . Using this equation, we can determine  $D_t$  from a plot of  $\ln(I/I_0)$  versus  $G^2$ .

**Dynamic Light Scattering Experiments.** The DLS experiments were performed using a He–Ne laser as a light source ( $\lambda = 632.8 \text{ nm}$ ), a photomultiplier as a detector, and a digital correlator (model ALV5000, ALV-Laser Vertriebsgesellschaft, Langen, Germany). The scattered light was detected at scattering angles  $\vartheta$  ranging from  $30^\circ$  to  $90^\circ$ . The polarization of the scattered light was selected to be parallel to the incident polarization. The capillary containing the investigated solution was placed into an index-matching bath to minimize scattering from the outer capillary wall.

We measured the normalized homodyne intensity correlation function  $g_2(t) = \langle I(0)I(t) \rangle / \langle I \rangle^2$  of the scattered light that probes the dynamical response of the system given as:<sup>35</sup>

$$g_2(t) = 1 + \left| \sum_i A_i \exp[-(t/\tau_i)^{\beta_i}] \right|^2 \quad (2)$$

where  $A_i$  is the amplitude and  $\tau_i$  is the relaxation time of the  $i$ -th relaxation mode. For a solution of nearly monodisperse scatterers, the Kohlrausch–Williams–Watts (KWW) parameter  $\beta_i$  is close to 1, while in solutions with polydisperse scattering objects smaller  $\beta_i$  values are obtained. The apparent translational diffusion coefficients were calculated as

$$D_t = 1/\tau q^2 \quad (3)$$

where  $q = (4\pi n/\lambda) \sin(\vartheta/2)$  is the scattering vector and  $n = 1.33$  is the refractive index of the solution.

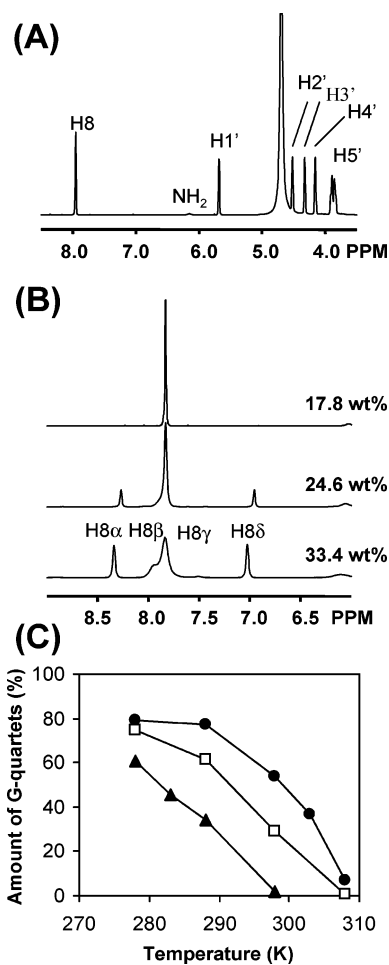


**Figure 2.** (A) Complete  $^1\text{H}$  NMR spectrum for 17.8 wt %  $\text{Na}_2(5'\text{-GMP})$  at 298 K. (B) Expansion of the H8 region for three concentrations at 298 K. (C) Degree of G-quartet aggregation as a function of  $\text{Na}_2(5'\text{-GMP})$  concentration and temperature. 17.8 wt % ( $\blacktriangle$ ), 24.6 wt % ( $\square$ ), 33.4 wt % ( $\bullet$ ).

## Results and Discussion

**$^1\text{H}$  NMR Spectra.** Figure 2 shows the full  $^1\text{H}$  NMR spectrum and the expanded H8 regions for  $\text{Na}_2(5'\text{-GMP})$  (pH 8) obtained at different concentrations. Spectral assignment for the H8 signals has been established from early NMR studies.<sup>8–18</sup> Specifically, H8 $\alpha$ , H8 $\delta$ , and H8 $\beta$  signals are attributed to the  $5'\text{-GMP}$  aggregates containing G-quartets, while H8 $\gamma$  arises from  $5'\text{-GMP}$  monomers or monomer aggregates. As seen from Figure 2, higher  $5'\text{-GMP}$  concentrations promote the formation of G-quartet aggregates. From the signal integrations for H8 $\alpha$ , H8 $\delta$ , and H8 $\beta$ , we can estimate the degree of G-quartet aggregation (i.e., relative population of G-quartet aggregates). Figure 2C shows the concentration and temperature dependencies of the formation of  $5'\text{-GMP}$  aggregates. For a given  $5'\text{-GMP}$  concentration, the curve shown in Figure 2C is reminiscent of a melting curve. If we define the “melting” temperature for  $5'\text{-GMP}$  self-assembly as the temperature at which the population of quartet aggregates is 50% of the total aggregates, the melting temperature for 17.8, 24.6, and 33.4 wt %  $\text{Na}_2(5'\text{-GMP})$  samples is approximately 283, 295, and 302 K, respectively. These melting temperatures are similar to those observed in the DLS study of  $\text{Na}_2(5'\text{-GMP})$ .<sup>19</sup> The high melting temperatures observed for high  $5'\text{-GMP}$  concentrations suggest that the aggregate size increases with  $5'\text{-GMP}$  concentration (vide infra).

(32) Wu, D.; Chen, A.; Johnson, C. S., Jr. *J. Magn. Reson., Ser. A* **1995**, *115*, 123–126.

(33) Piatto, M.; Saudek, V.; Slenar, V. *J. Biomol. NMR* **1992**, *2*, 661–665.

(34) (a) Stejskal, E. O.; Tanner, J. E. *J. Chem. Phys.* **1965**, *42*, 288–292. (b) Tanner, E. J. *J. Chem. Phys.* **1970**, *52*, 2523–2526.

(35) (a) Berne, B. J.; Pecora, R. *Dynamic Light Scattering*; Wiley: New York, 1976. (b) Schmitz, K. S. *An Introduction to Dynamic Light Scattering by Macromolecules*; Academic Press: San Diego, CA, 1990.

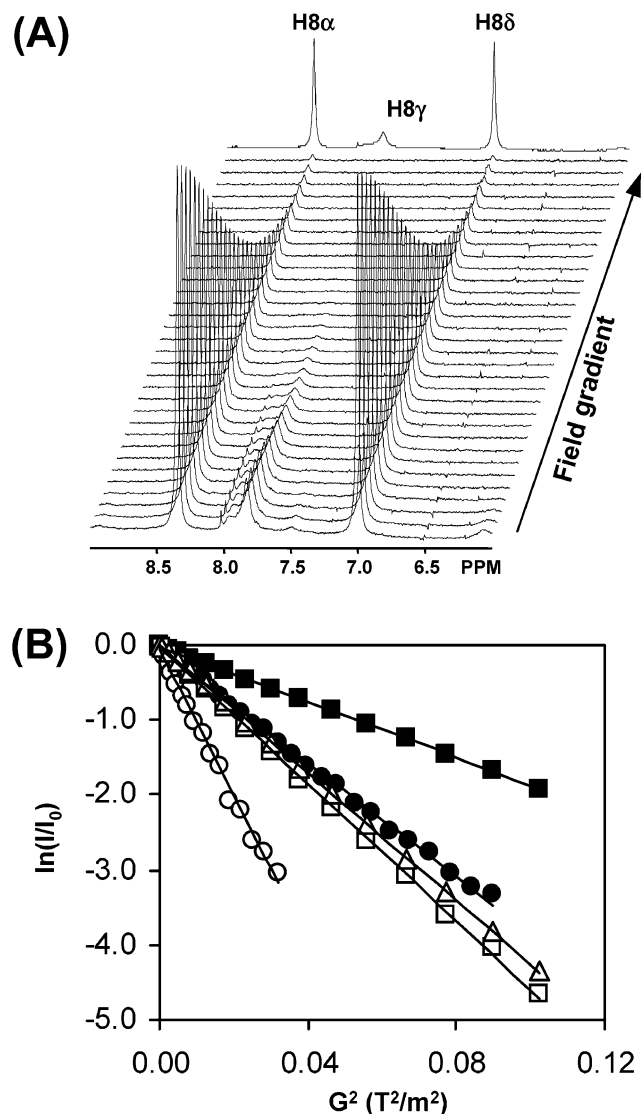


**Figure 3.** (A) Stack plot of <sup>1</sup>H NMR spectra from the diffusion experiment for Na<sub>2</sub>(5'-GMP) (33.4 wt %) at 298 K. (B) Plots of diffusion data for Na<sub>2</sub>(5'-GMP) at three different concentrations: 17.8 wt % (△), 24.6 wt % (□, ■), and 33.4 wt % (○, ●). Data for stacking monomers and stacking quartets are represented by open and filled symbols, respectively.

**NMR Diffusion Experiments.** Although the <sup>1</sup>H NMR spectra shown in Figure 2 contain valuable information about stoichiometric distributions of different molecular species present in solution, they cannot yield information about the geometrical size for the two types of 5'-GMP aggregates. In this work, we performed extensive <sup>1</sup>H NMR experiments to measure translational diffusion coefficients (*D<sub>t</sub>*) for the 5'-GMP aggregates. From the observed *D<sub>t</sub>* values, it is then possible to obtain information about the aggregate size, as will be discussed further in the next section. One of the advantages of NMR diffusion experiments is that *D<sub>t</sub>* can be determined separately for G-quartet aggregates (H8α and H8δ signals) and for monomer aggregates (H8γ signal). The concentration for the molecular species associated with the H8β signal is negligible.

Figure 3 shows the results from a typical NMR diffusion experiment for Na<sub>2</sub>(5'-GMP). The complete NMR diffusion data obtained for Na<sub>2</sub>(5'-GMP) at various concentrations and temperatures are summarized in Tables 1 and 2. In general, the value of *D<sub>t</sub>* is significantly larger for the monomer aggregates

than that for the G-quartet aggregates. This suggests that the latter species has a much larger size. In principle, the two types of aggregates undergo chemical exchange, which may potentially complicate the interpretation for the observed NMR diffusion data. However, the chemical exchange among 5'-GMP aggregates is known to be much slower than the NMR diffusion time scale.<sup>8</sup> In addition, the bipolar LED pulse sequence is insensitive to chemical exchange modulation.<sup>36</sup> For these reasons, chemical exchange can be safely ignored in the present study. As seen from Table 1, in dilute Na<sub>2</sub>(5'-GMP) samples (below 17.8 wt %), only stacking monomers can be detected at room temperature. Under these circumstances, our data are in excellent agreement with the previously reported *D<sub>t</sub>* values, 3.57 to 1.74 × 10<sup>-10</sup> m<sup>2</sup>·s<sup>-1</sup> for 5'-GMP in a concentration range from 0.0344 to 0.363 M.<sup>31</sup> As also seen from Figure 3, the NMR diffusion data shows excellent linearity. This immediately suggests that both types of 5'-GMP aggregates exhibit very good monodispersity.

**A Combined Hydrodynamic Model.** In this section, we describe a hydrodynamic model for interpreting the experimental *D<sub>t</sub>* data. According to hydrodynamic theory, the isotropic translational diffusion coefficient, *D<sub>t</sub>*, for a symmetric cylinder of length *L* and diameter *d* can be written as:

$$D_t = \frac{kT}{3\pi\eta L}(\ln p + \nu) \quad (4)$$

where *kT* is the Boltzmann factor, *η* is the solvent viscosity, *p* is the axial ratio of the cylinder (*p* = *L/d*), and *ν* is known as the end-effect correction term. For symmetric cylinders with 2 ≤ *p* ≤ 30, Tirado and Garcia de la Torre obtained the following approximate expression for the end-effect correction:<sup>37-39</sup>

$$\nu = 0.312 + 0.565p^{-1} - 0.100p^{-2} \quad (5)$$

Using eqs 4 and 5, one can obtain information about *p* from *D<sub>t</sub>*. This is known as the cylinder model of Tirado and Garcia de la Torre. Furthermore, if the cylinder diameter, *d*, is known for a particular system, the only variable to be determined is the length of the cylinder, *L*. For cylinders formed by 5'-GMP self-association, the diameters for monomer aggregates and G-quartet aggregates are known to be 10 and 26 Å, respectively.<sup>20</sup> However, one limitation of the cylinder model is that eqs 4 and 5 are valid only for cylinders with 2 ≤ *p* ≤ 30. For short cylinders (*p* < 2), Jurga-Nowak et al.<sup>20</sup> recently demonstrated that the bead model works better than the cylinder model. Thus in this study we used a combined hydrodynamic model that couples the cylinder model with the bead model. As illustrated in Figure 4, we used the cylinder model to analyze situations with *p* > 2 and the bead model to treat cylinders with *p* < 2. It should be mentioned that the cylinder model is valid for the majority of the cases examined in the present study. Using this combined model, we obtained the geometrical size for the cylinders composed of stacking monomers and stacking G-quartets (Table 1). For both types of aggregates, the spacing

(36) Chen, A.; Johnson, C. S., Jr.; Lin, M.; Shapiro, M. J. *J. Am. Chem. Soc.* **1998**, *120*, 9094–9095.

(37) Tirado, M. M.; Garcia de la Torre, J. *J. Chem. Phys.* **1979**, *71*, 2581–2587.

(38) Tirado, M. M.; Garcia de la Torre, J. *J. Chem. Phys.* **1980**, *73*, 1986–1993.

(39) Tirado, M. M.; Lopez Martinez, C.; Garcia de la Torre, J. *J. Chem. Phys.* **1984**, *81*, 2047–2052.

**Table 1.** Experimental NMR Translational Diffusion Coefficients ( $D_t$ )<sup>a</sup> and Sizes for Na<sub>2</sub>(5'-GMP) Self-Assemblies

concentration (wt %)	population of G-quartets (%) <sup>b</sup>	stacking monomers				stacking quartets			
		$D_t$	$n$	$L$ (nm)	$p$	$D_t^c$	$n$	$L$ (nm)	$p$
17.8	0	1.98	11 ± 1	3.4	3.4	—	—	—	—
24.6	29	1.42	19 ± 1	6.1	6.1	0.55	48 ± 3	16.0	6.15
28.9	44	1.18	26 ± 1	8.5	8.5	0.47	62 ± 5	20.7	7.96
33.4	53	0.98	34 ± 2	11.2	11.2	0.38	87 ± 8	29.2	11.2

<sup>a</sup> Measured in D<sub>2</sub>O at 298 K. All  $D_t$  values are in units of 10<sup>-10</sup> m<sup>2</sup>/s. The uncertainty in  $D_t$  was estimated to be ±0.04 × 10<sup>-10</sup> m<sup>2</sup>/s. <sup>b</sup> Determined from relative signal areas for H8 signals. <sup>c</sup> Averaged value between those measured for H8α and H8δ signals.

**Table 2.** Experimental NMR Translational Diffusion Coefficients ( $D_t$ )<sup>a</sup> for Na<sub>2</sub>(5'-GMP) Self-Assemblies at Various Temperatures

	temp (K)	stacking monomers				stacking quartets			
		$D_t$	$n$	$L$ (nm)	$p$	$D_t$	$n$	$L$ (nm)	$p$
17.8 wt %	293	1.84	9 ± 1	2.7	2.7	0.68	24 ± 2	7.8	3.00
	288	1.47	11 ± 1	3.4	3.4	0.63	24 ± 2	7.8	3.00
	283	1.13	13 ± 1	4.1	4.1	0.50	24 ± 2	7.8	3.00
	278	0.88	14 ± 1	4.4	4.4	0.38	24 ± 2	7.8	3.00
24.6 wt %	298	1.42	19 ± 1	6.1	6.1	0.55	48 ± 3	16.0	6.15
	293	1.13	22 ± 1	7.1	7.1	0.45	48 ± 3	16.0	6.15
	288	0.90	24 ± 1	7.8	7.8	0.40	48 ± 3	16.0	6.15
	283	0.72	27 ± 2	8.8	8.8	0.33	48 ± 3	16.0	6.15
	278	0.59	27 ± 2	8.8	8.8	0.25	48 ± 3	16.0	6.15

<sup>a</sup> Measured for Na<sub>2</sub>(5'-GMP) in D<sub>2</sub>O. All  $D_t$  values are in units of 10<sup>-10</sup> m<sup>2</sup>/s. The uncertainty in  $D_t$  was estimated to be ±0.04 × 10<sup>-10</sup> m<sup>2</sup>/s.

between two adjacent stacks is 3.4 Å.<sup>20</sup> The length of the cylinder,  $L$ , is equal to  $(n - 1) \times 0.34$  nm, where  $n$  is the number of stacks in each cylinder.

**Effect of Concentration and Temperature.** As seen from Table 1, the size of both monomer and quartet aggregates increases with concentration. This is in agreement with the observed melting behaviors discussed earlier. The largest G-quartet aggregate found in this study is composed of a stack of 87 quartets forming a cylinder of 29.2 nm. Such nanoscale aggregates are significantly larger than what has been believed for Na<sub>2</sub>(5'-GMP) self-assembly at pH 8. It is also interesting to see from Table 1 that aggregates composed of stacking 5'-GMP monomers can have a considerably large size as well. In this study, the accuracy in the reported aggregate size is derived from the standard deviation of the experimental NMR diffusion data. If systematic errors were considered, the actual errors in the estimated aggregate size may be greater than those reported.

To obtain further information about Na<sub>2</sub>(5'-GMP) aggregation, we also performed NMR diffusion measurements for two Na<sub>2</sub>(5'-GMP) samples (17.8 and 24.6 wt %) at different

temperatures. As seen from Table 2, the magnitude of  $D_t$  generally decreases with temperature. However, this does not necessarily mean that the aggregate size must be increased as temperature decreases. To properly analyze the variable temperature  $D_t$  data, we must also take into consideration the temperature dependence of solvent viscosity,  $\eta$  (see eq 4). In this study, we use the following relationship to describe the temperature effect for D<sub>2</sub>O:<sup>40</sup>

$$\log \eta(\text{D}_2\text{O}) = -1.2911 - \frac{164.97}{174.24 - T} \quad (6)$$

where the unit for  $\eta$  is centipoise (cP, 1 cP = 0.001 kg m<sup>-1</sup> s<sup>-1</sup>). Combining eqs 4–6, we were able to determine the size for the 5'-GMP cylinders at different temperatures (Table 2). It is quite surprising to see from Table 2 that, whereas the size of the monomer aggregates shows a small but notable increase in the temperature range from 298 to 278 K, the size of the quartet aggregates is essentially independent of the temperature. These temperature dependencies are best illustrated in a Stokes–Einstein (SE) plot ( $D_t$  versus  $T/\eta$ ), as shown in Figure 5. As predicted by eq 4, if the aggregate size is independent of temperature, a straight line should be observed in the SE plot. It is clearly seen from Figure 5 that, while the data for quartet aggregates lie on straight lines, the data for monomer aggregates show an upward curvature.

Although the monomer aggregates and quartet aggregates have quite different sizes, we found strong evidence that the two types of aggregation processes are intrinsically related. As illustrated in Figure 6, a plot of the axial ratio of the cylinder,  $p = L/d$ , against Na<sub>2</sub>(5'-GMP) concentration exhibits a nice linear relationship for both types of 5'-GMP aggregates. This somewhat surprising observation may imply that the same mechanism is operative for the stacking of monomers and the stacking of G-quartets. This is an interesting proposal, because it has been long believed that stacking of G-quartets is more

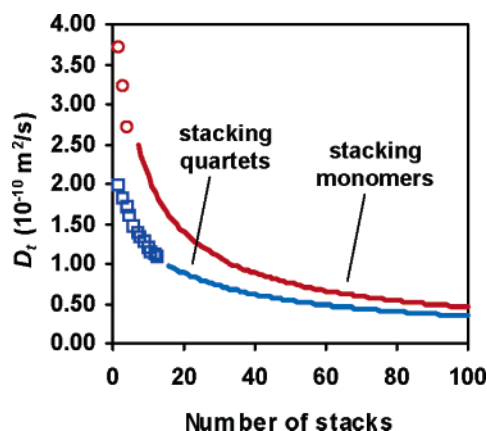


**Figure 4.** Combined hydrodynamic model for relating translational diffusion coefficient to number of stacking G-quartets. Bead model (symbols) and cylinder model (solid curve). The  $D_t$  values used in the model correspond to those determined in D<sub>2</sub>O at 298 K.

(40) Lapham, J.; Rife, J. P.; Moore, P. B.; Crothers, D. M. *J. Biomol. NMR* **1997**, *10*, 255–262.

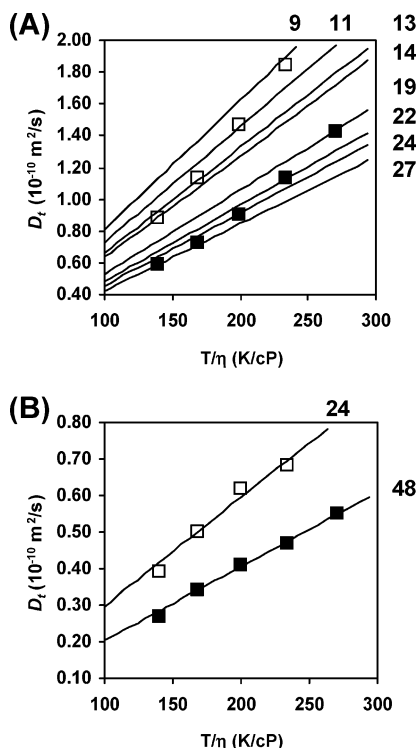


**Figure 5.** Stokes–Einstein (SE) plot for (A) monomer aggregates and (B) quartet aggregates at two Na<sub>2</sub>(5'-GMP) concentrations: 17.8 wt % (□) and 24.6 wt % (■).

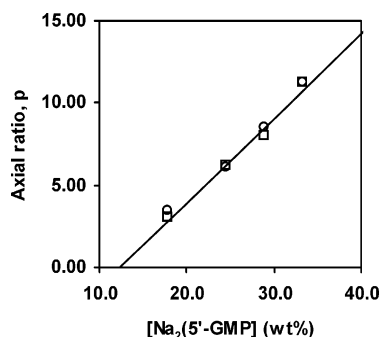


**Figure 6.** Linear relationship between axial ratio and Na<sub>2</sub>(5'-GMP) concentration for monomer aggregates (○) and quartet aggregates (□).

avored than stacking of guanine monomers. However, the linear relationship shown in Figure 6 suggests that the reason for the formation of longer quartet aggregates is because the diameter of the G-quartet (so the ability to form  $\pi$  stacking) is greater than that of a single guanine molecule. It appears that the  $\pi$  stacking is the predominant force to induce 5'-GMP aggregates along the axial direction. The function of the monovalent cations is simply to stabilize the G-quartet structure via the ion–dipole interaction. Some crystallographic evidence seems to support this viewpoint. For example, there are cases where two G-quartets are stacked on top of one another with a void central cavity, as observed in both G-DNA oligomers<sup>41–43</sup> and self-assembled guanosine systems.<sup>44,45</sup> Of course, the current analysis is based on the assumption that both monomer and G-quartet

aggregates can be modeled as cylinders. Whereas crystallographic evidence warrants the use of a cylinder model for describing G-quartet aggregates, the detailed structural information for monomer aggregates is unavailable. At high 5'-GMP concentrations, it is possible that the overall structure of a monomer aggregate deviates considerably from a cylinder shape. Nevertheless, it would be of importance to further investigate the different roles that base stacking and ion–dipole interactions play in the 5'-GMP aggregation process.

**Solvent Isotope Effect.** In general, NMR diffusion experiments are performed for samples dissolved in D<sub>2</sub>O. However, Borzo et al.<sup>12</sup> observed that the melting temperature of Na<sub>2</sub>(5'-GMP) aggregates is slightly higher in D<sub>2</sub>O than in H<sub>2</sub>O. In this section, we attempt to address the question as to how the size of 5'-GMP aggregates depends on the isotope composition of the aqueous solution. As seen from Table 3, we measured  $D_t$  values for Na<sub>2</sub>(5'-GMP) (24.6 wt %) in aqueous solutions with a different H<sub>2</sub>O/D<sub>2</sub>O mix. In general, the magnitude of  $D_t$  decreases with an increase of the D<sub>2</sub>O content in the solvent. However, similar to the analysis of variable temperature  $D_t$  data, it is also critical to know the viscosity for the mixed H<sub>2</sub>O/D<sub>2</sub>O solvent before the experimental  $D_t$  data can be properly interpreted. Fortunately, previous studies have shown that the viscosity of a H<sub>2</sub>O/D<sub>2</sub>O mixture can be calculated from the viscosity of pure liquids at the same temperature and pressure from the following simple linear relation:<sup>46</sup>

$$\eta_{\text{H}_2\text{O}+\text{D}_2\text{O}}(T,P) = \chi_{\text{H}_2\text{O}}\eta_{\text{H}_2\text{O}}(T,P) + \chi_{\text{D}_2\text{O}}\eta_{\text{D}_2\text{O}}(T,P) \quad (7)$$

where  $\chi$  represents the mole fraction of the solvent component,  $\eta(\text{H}_2\text{O}) = 0.8920$  cP and  $\eta(\text{D}_2\text{O}) = 1.097$  cP at 298 K and 1 atm pressure. Using the correct solvent viscosity, we determined the sizes for the 5'-GMP aggregates. It is seen from Table 3 that, while the monomer aggregates do not exhibit any solvent isotope effect, the quartet aggregates have a larger size in D<sub>2</sub>O than in H<sub>2</sub>O or mixed solvents. This observation is in line with the prediction based on the solvent isotope effect on hydrogen bonding, because hydrogen bonding is the most important difference between the two types of 5'-GMP aggregates. On the other hand, it is speculated that hydrophobic interactions such as  $\pi$  stacking may also play a role in the formation of 5'-GMP aggregates.<sup>47</sup>

**Effect of Added Salt.** It is known from previous studies that adding salt (monovalent cations) into 5'-GMP solution can strongly change the formation of 5'-GMP aggregates. Very often, previous studies focused on competition or synergy between two different types of cations such as K<sup>+</sup>/NH<sub>4</sub><sup>+</sup> or Na<sup>+</sup>/K<sup>+</sup>. Because the surface and cavity of the 5'-GMP aggregates exhibit quite different binding affinities for various monovalent cations,<sup>48</sup> the presence of two or more types of cations often results in complicated effects. Sometimes it is desirable to have more than one type of cations present in solution so that one can use them to control the aggregation process. One example is the control of G2-DNA and G4-DNA formation by changing the Na<sup>+</sup>/K<sup>+</sup> ratio in solution, so-called the “Na<sup>+</sup>–K<sup>+</sup> switch”.<sup>49</sup>

(41) Laughlan, G.; Murchie, A. I. H.; Norman, D. G.; Moore, M. H.; Moody, P. C. E.; Lilley, D. M. J.; Luisi, B. *Science (Washington, D.C.)* **1994**, *265*, 520–524.  
 (42) Phillips, K.; Dauter, Z.; Murchie, A. I. H.; Lilley, D. M. J.; Luisi, B. *J. Mol. Biol.* **1997**, *273*, 171–182.  
 (43) Horvath, M. P.; Schultz, S. C. *J. Mol. Biol.* **2001**, *310*, 367–377.  
 (44) Kotch, F. W.; Fetting, J. C.; Davis, J. T. *Org. Lett.* **2000**, *2*, 3277–3280.

(45) Shi, X.; Fetting, J. C.; Davis, J. T. *J. Am. Chem. Soc.* **2001**, *123*, 6738–6739.  
 (46) Kestin, J.; Imaishi, N.; Nott, S. H.; Nieuwoudt, J. C.; Sengers, J. V. *Physica* **1985**, *134A*, 38–58.  
 (47) Carughi, F.; Ceretti, M.; Mariani, P. *Eur. Biophys. J.* **1992**, *21*, 155–161.  
 (48) Wong, A.; Wu, G. *J. Am. Chem. Soc.* **2004**, *125*, 13895–13905.  
 (49) Sen, D.; Gilbert, W. *Nature* **1990**, *344*, 364–366.

**Table 3.** Solvent Isotope Effect on the Size of Na<sub>2</sub>(5'-GMP) (24.6 wt %) Self-Assemblies at 298 K<sup>a</sup>

solvent	solvent viscosity <sup>b</sup>	stacking monomers			stacking quartets		
		D <sub>t</sub>	n	L (nm)	D <sub>t</sub> <sup>c</sup>	n	L (nm)
H <sub>2</sub> O	0.8929	1.72	20 ± 1	6.5	0.75	40 ± 2	13.3
H <sub>2</sub> O/D <sub>2</sub> O (80:20)	0.9322	1.70	19 ± 1	6.1	0.72	40 ± 2	13.3
H <sub>2</sub> O/D <sub>2</sub> O (40:60)	1.016	1.60	18 ± 1	5.8	0.65	41 ± 2	13.6
D <sub>2</sub> O	1.097	1.42	19 ± 1	6.1	0.55	48 ± 2	16.0

<sup>a</sup> All D<sub>t</sub> values are expressed in units of 10<sup>-10</sup> m<sup>2</sup>/s. The uncertainty in D<sub>t</sub> was estimated to be ±0.04 × 10<sup>-10</sup> m<sup>2</sup>/s. <sup>b</sup> Calculated using eq 7. <sup>c</sup> Averaged value between those measured for H8α and H8δ signals.

**Table 4.** Experimental NMR Translational Diffusion Coefficients (D<sub>t</sub>)<sup>a</sup> for Na<sub>2</sub>(5'-GMP) Self-Assemblies in Different Salt Solutions

[NaCl]	population of G-quartets (%) <sup>b</sup>	stacking monomers			stacking quartets		
		D <sub>t</sub>	n	L (nm)	D <sub>t</sub>	n	L (nm)
0	0	1.98	11 ± 1	3.4	—	—	—
100 mM	1	2.13	10 ± 1	3.1	0.74	28 ± 2	9.2
250 mM	7	2.02	11 ± 1	3.4	0.78	26 ± 2	8.5
500 mM	15	1.95	11 ± 1	3.4	0.79	26 ± 2	8.5

<sup>a</sup> Measured for 17.8 wt % Na<sub>2</sub>(5'-GMP) in D<sub>2</sub>O at 298 K. All D<sub>t</sub> values are in units of 10<sup>-10</sup> m<sup>2</sup>/s. The uncertainty in D<sub>t</sub> was estimated to be ±0.04 × 10<sup>-10</sup> m<sup>2</sup>/s. <sup>b</sup> Determined from relative signal areas for H8 signals.

**Table 5.** Comparison of Translational Diffusion Coefficients (D<sub>t</sub>)<sup>a</sup> Determined by NMR and DLS Experiments for Na<sub>2</sub>(5'-GMP) in H<sub>2</sub>O

c (wt %)	NMR experiment				DLS experiment <sup>b</sup>	
	D <sub>t</sub> (monomers) <sup>c</sup>	D <sub>t</sub> (quartets) <sup>c</sup>	D <sub>t</sub> (average)	β	c (wt %)	D <sub>t</sub>
17.8	2.43	—	—	—	18	3.24 ± 0.09
24.6	1.74	0.65	1.335	0.964	25	1.14 ± 0.05
28.9	1.45	0.58	0.983	0.956	30	1.02 ± 0.02
33.4	1.20	0.47	0.738	0.950		

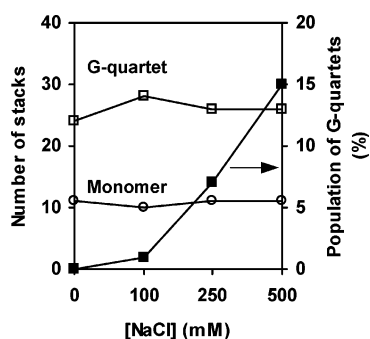
<sup>a</sup> All D<sub>t</sub> values are expressed in units of 10<sup>-10</sup> m<sup>2</sup>/s. <sup>b</sup> DLS experiments were performed at 296 K and pH 7.7. <sup>c</sup> Calculated from the D<sub>t</sub> values experimentally determined in D<sub>2</sub>O using eq 9.

However, our goal in the present study is to avoid complication arising from competition or synergy between different types of cations. For this reason, we examined the salt effect by adding Na<sup>+</sup> into Na<sub>2</sub>(5'-GMP). The results are presented in Table 4. The influence of added NaCl on the solvent viscosity can be corrected by using the following equation:<sup>40</sup>

$$\eta = \eta_0(1 + 0.0067 \times \sqrt{[\text{NaCl}]} + 0.0244 \times [\text{NaCl}]) \quad (8)$$

where  $\eta_0$  is the solvent viscosity in the absence of NaCl. This salt correction term is generally small (e.g., at 500 mM NaCl,  $\eta = 1.017\eta_0$ ). As seen from Figure 7, the added NaCl increases the population of G-quartet aggregates but has little effect on the sizes of both monomer and quartet aggregates.

**Dynamic Light Scattering.** To obtain an independent evaluation for the size of Na<sub>2</sub>(5'-GMP) aggregates at pH 8, we also performed DLS experiments at Na<sub>2</sub>(5'-GMP) concentrations similar to those used in the NMR experiments. The DLS results

**Figure 7.** Size and population of Na<sub>2</sub>(5'-GMP) aggregates as a function of added NaCl.

are shown in Table 5. However, there are two major issues that need to be addressed before it is possible to compare DLS data with NMR data. First, because the DLS experiments were performed for Na<sub>2</sub>(5'-GMP) samples dissolved in H<sub>2</sub>O, the observed D<sub>t</sub>(DLS) data cannot be directly compared with the corresponding NMR data, D<sub>t</sub>(NMR), which were measured for samples dissolved in D<sub>2</sub>O. To facilitate a meaningful comparison, we converted the experimental NMR diffusion data, D<sub>t</sub>(D<sub>2</sub>O), to the “expected” values for D<sub>t</sub>(H<sub>2</sub>O) using the following equation:

$$D_t(\text{H}_2\text{O}, 296 \text{ K}) = D_t(\text{D}_2\text{O}, 298 \text{ K}) \frac{296 \text{ K} \times \eta(\text{H}_2\text{O}, 296 \text{ K})}{298 \text{ K} \times \eta(\text{D}_2\text{O}, 298 \text{ K})} \quad (9)$$

The underlying assumption in the above equation is that the aggregate sizes are the same in H<sub>2</sub>O and in D<sub>2</sub>O. However, in the previous section, we described a small solvent isotope effect for quartet aggregates. Nonetheless, because of the qualitative nature of the discussion presented in this section, we ignore this small solvent isotope effect. The second issue is more significant. On the basis of NMR data, we know that there exist two types of molecular aggregates in Na<sub>2</sub>(5'-GMP) solution. Because of the similarity between the two types of molecular species, all experimental DLS curves can be perfectly fitted by a single exponential function, which yields only one D<sub>t</sub> value. As seen from Table 5, the magnitude of D<sub>t</sub>(DLS) data is intermediate between D<sub>t</sub>(monomers) and D<sub>t</sub>(quartets). This strongly suggests that DLS data reflect an averaged effect.

In the discussion that follows, we describe a procedure that allows us to obtain an averaged D<sub>t</sub> value from the experimentally



**Table 6.** Comparison of Translational Diffusion Coefficients and Molecular Dimensions Observed for 5'-GMP Self-Assemblies and G-Quadruplexes Formed by Telomeric DNA Oligomers

system	method	$D_t$ ( $10^{-10}$ m <sup>2</sup> /s)	$n^a$	$L^b$ (nm)	ref
d(TTGGGGTTGGGGTT) bimolecular hairpin quadruplex	DLS	1.48	$5.5 \pm 0.5$	1.53	26
d(GGTTGGTGTGGTTGG) unimolecular quadruplex	DLS	1.8	$3 \pm 0.5$	0.68	26
d(TTGGGGTT) bimolecular quadruplex	DLS	1.34	$6.8 \pm 0.5$	1.97	26
d(TGGGGT) <sub>4</sub> unimolecular quadruplex	DLS	1.4	$6.2 \pm 0.5$	1.77	50
tetramolecular quadruplex	DLS	0.8	$19 \pm 1$	6.1	50
Na <sub>2</sub> (5'-GMP), pH 8					
24.6 wt %	NMR	0.55	$48 \pm 3$	16.0	this work
28.9 wt %	NMR	0.47	$62 \pm 5$	20.7	this work
33.4 wt %	NMR	0.38	$87 \pm 8$	29.2	this work

<sup>a</sup> Because the  $D_t$  data from the DLS experiments were reported as  $D_t(\text{H}_2\text{O}, 293 \text{ K})$  (also known as  $D_t^{20}$ ), they need to be converted using  $D_t(\text{D}_2\text{O}, 298 \text{ K}) = 1.113 \times D_t(\text{H}_2\text{O}, 293 \text{ K})$  before one can use the combined hydrodynamic model shown in Figure 4 to determine  $n$ . <sup>b</sup>  $L = (n - 1) \times 0.34 \text{ nm}$ .

determined  $D_t$  data for monomer aggregates and quartet aggregates. The procedure consists of two steps. (1) We use  $D_t$ - (monomer) and  $D_t$ (quartet) listed in Table 5 to calculate the relaxation times in the expected "experimental" DLS curve using eq 10. The amplitude of each relaxation mode was

$$g_2(t) = [A_m \exp(-t/\tau_m) + A_t \exp(-t/\tau_t)]^2 + 1 \quad (10)$$

weighted by the degree of aggregation of the corresponding species determined by NMR (Table 1). (2) We then use a single-exponential decay to fit the "experimental" DLS curve. To determine the deviation from pure monodispersity, the KWW parameter  $\beta$  was used ( $\beta = 1$  for pure monodisperse scatters). From the obtained relaxation time the averaged diffusion coefficient,  $D_t$ (average), was obtained. As seen from Table 5, a qualitative agreement is observed between NMR and DLS data. Considering the number of oversimplified assumptions used in the above analysis, the observed agreement between the NMR and DLS data provides strong evidence to support our evaluation of the 5'-GMP aggregate size. It is also noted in Table 5 that the NMR and DLS results are different even for the low concentration sample (17.8%) where only monomer aggregates are present. The precise reason for this discrepancy was unclear. However, because the NMR and DLS experiments were not conducted for the same samples and under identical conditions, the conclusion drawn from this section should be considered to be only qualitative.

**Na<sub>2</sub>(5'-GMP) Supramolecular Structure and Telomeric DNA.** As we have discussed in the previous sections, the stacking of individual G-quartets in Na<sub>2</sub>(5'-GMP) aggregates can form a 30-nm-long molecular cylinder. The overall shape of such a cylinder is very similar to those of G-quadruplexes formed by telomeric DNA sequences. The major difference is that, in G-quadruplexes, all G-quartets from a single strand are linked by a DNA backbone. Because telomeric DNA G-quadruplexes form well-defined folding structures, they serve as excellent models for testing the validity of our hydrodynamic model. Table 6 gives a summary of the translational diffusion coefficients determined for G-quadruplexes formed by telomeric DNA oligomers. The molecular dimensions shown in Table 6 were obtained by using the combined hydrodynamic model described earlier.

The 15-mer DNA, d(GGTTGGTGTGGTTGG), is known as the thrombin binding aptamer (TBA), which folds into a

unimolecular quadruplex in the presence of K<sup>+</sup>.<sup>51–53</sup> The quadruplex structure consists of two stacking G-quartets and three loops, as shown in Figure 8A. As seen from Table 6, the

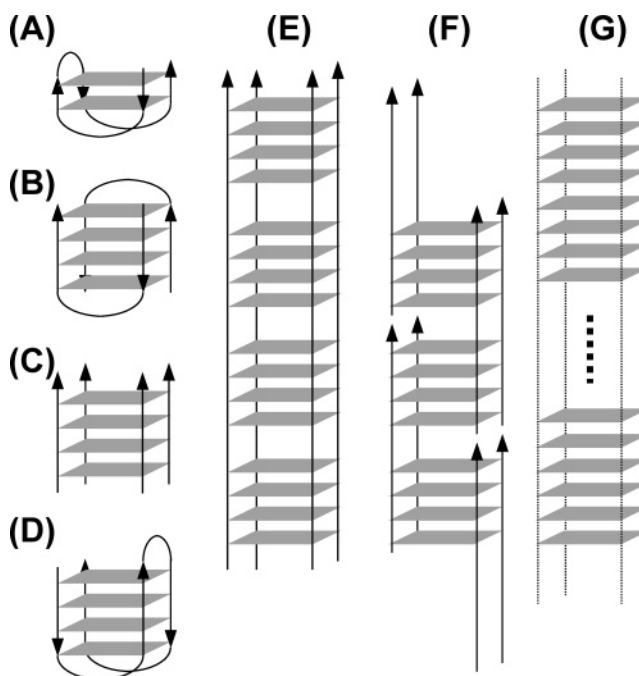


**Figure 8.** Schematic illustration of various forms of G-quadruplex structure. (A, D) Unimolecular quadruplex. (B) Bimolecular hairpin quadruplex. (C, E) Tetramolecular parallel quadruplex. (F) G-wire. (G) 5'-GMP self-assembly.

value of  $D_t$  observed for this DNA is  $1.8 \times 10^{-10}$  m<sup>2</sup>/s. Using the combined hydrodynamic model, we determined that the length of this quadruplex is equivalent to three stacking G-quartets,  $L = 0.68 \text{ nm}$ . Because there are only two stacking G-quartets in d(GGTTGGTGTGGTTGG), the extra length ( $n = 3.0 - 2 = 1.0$ ) must be contributed by the T2 loops. With such a short cylinder length ( $p = L/d = 0.68/2.6 = 0.26$ ), the folded structure of d(GGTTGGTGTGGTTGG) looks more like a disk than a cylinder.

- (50) Włodarczyk, A.; Gapinski, J.; Patkowski, A.; Dobek, A. *Acta Biochim. Pol.* **1999**, *46*, 609–613.  
 (51) Wang, K. Y.; McCurdy, S.; Shea, R. G.; Swaminathan, S.; Bolton, P. H. *Biochemistry* **1993**, *32*, 1899–1904.  
 (52) Macaya, R. F.; Schultze, P.; Smith, F. W.; Roe, J. A.; Feigon, J. *Proc. Natl. Acad. Sci. U.S.A.* **1993**, *90*, 3745–3749.  
 (53) Schultze, P.; Macaya, R. F.; Feigon, J. *J. Mol. Biol.* **1994**, *235*, 1532–1547.

Both d(TTGGGGTT) and d(TTGGGGTTGGGGTT) are related to the telomeric repeat from *Tetrahymena* chromosome, TTGGGG. Although these two DNA oligomers have very different lengths, the observed  $D_t$  values are quite similar, 1.34 and  $1.48 \times 10^{-10}$  m<sup>2</sup>/s, suggesting that the folded structures for these two DNA molecules have similar overall shapes. Bolten et al.<sup>26</sup> interpreted these  $D_t$  data as evidence that d(TTGGGGTTGGGGTT) forms a bimolecular hairpin quadruplex (Figure 8B) and d(TTGGGGTT) is a tetramolecular parallel quadruplex (Figure 8C). Using our hydrodynamic model, we determined the length for d(TTGGGGTT) and d(TTGGGGTTGGGGTT) to be 1.97 and 1.53 nm, respectively. It should be noted that both quadruplex structures consist of four stacking G-quartets. Similar to the case in TBA, the extra length ( $n = 5.5 - 4.0 = 1.5$ ) observed in the d(TTGGGGTTGGGG) hairpin quadruplex is due to the presence of T2 loops. In contrast, the extra length is significantly larger in the tetramolecular parallel quadruplex d(TTGGGGTT),  $n = 6.8 - 4.0 = 2.8$ . This strongly suggests the formation of at least one T-quartet at each end of d(TTGGGGTT), similar to the situation observed in d(TTGGGGTT).<sup>54</sup>

Włodarczyk et al.<sup>50</sup> used PCS to study another *Tetrahymena* telomeric DNA repeat, d(TGGGGTTGGGGTTGGGGTTGGGGTT). They observed that two types of quadruplexes coexist in solution in the presence of Na<sup>+</sup>. On the basis of experimental  $D_t$  values and the bead model, they interpreted the  $D_t$  data as arising from unimolecular (Figure 8D) and tetramolecular (Figure 8E) quadruplexes. Using our combined model, we found that the length for the unimolecular quadruplex is 1.77 nm ( $n = 6.2$ ). This value is slightly longer than that of the hairpin quadruplex formed by d(TTGGGGTT). For the tetramolecular quadruplex, the length of the molecular cylinder is 6.1 nm ( $n = 19$ ) (Figure 8E). This size is consistent with the presence of 16 G-quartets and three T2 joints in this quadruplex. These results for the well-defined DNA G-quadruplexes further confirm that the combined hydrodynamic model is valid for interpreting the experimental  $D_t$  data. As seen from Table 6, the Na<sub>2</sub>(5'-GMP) aggregates are significantly larger than the listed DNA oligomers. However, it should also be noted that the 5'-GMP concentrations (ca. 0.5–1.0 M) are much higher than those for the DNA oligomers (typically just a few millimolar). At higher DNA strand concentrations, telomeric DNA oligomers can also form high molecular weight aggregates. In the case of the G-wires formed by d(GGGGTTGGGG) (Figure 8F), the aggregates can be as long as 1000 nm.<sup>27</sup>

## Conclusions

We have studied the geometrical size of Na<sub>2</sub>(5'-GMP) supramolecular structures at pH 8 by a combination of diffusion NMR and DLS methods. The results from these two different

techniques have firmly established that Na<sub>2</sub>(5'-GMP) aggregates are on the nanometer scale. Because 5'-GMP represents the simplest case for nucleotide self-association processes, the findings in this study may have important implications for understanding mechanism and structure in DNA or RNA superstructures. The nanoscale structure and morphology observed for Na<sub>2</sub>(5'-GMP) at relatively high concentrations can be considered to be an intermediate state between isotropic solution and liquid-crystalline DNA phase. The observed self-assembled behaviors of Na<sub>2</sub>(5'-GMP) under various conditions may provide insights into DNA packing in cells and eventually biological functions of G-quadruplex structures. In a broader context, the present work also illustrates the useful utility of diffusion NMR spectroscopy in supramolecular chemistry. One advantage of diffusion NMR over DLS is that aggregates with similar sizes can be measured simultaneously by NMR. Using diffusion data reported for telomeric DNA oligomers with well-defined folding structures in solution, we have confirmed the validity of the combined hydrodynamic model. The major conclusions about Na<sub>2</sub>(5'-GMP) aggregation at pH 8 are outlined below.

(i) The length of the molecular cylinder formed by stacking G-quartets is 8–30 nm for Na<sub>2</sub>(5'-GMP) concentrations between 18 and 33 wt %. Another type of aggregate is composed of stacking 5'-GMP monomers and has a considerably shorter length, 3–11 nm, for the same Na<sub>2</sub>(5'-GMP) concentrations. These nanoscale Na<sub>2</sub>(5'-GMP) aggregates are significantly larger than what has been believed for many years.

(ii) We have found that, while the length of the monomer aggregates increases slightly with temperature, the length of the quartet aggregates is essentially independent of temperature.

(iii) We have found that, at a given Na<sub>2</sub>(5'-GMP) concentration, the monomer aggregates and quartet aggregates form molecular cylinders with the same axial ratio. This can be considered as strong evidence suggesting that the same stacking mechanism is in action for both types of aggregates.

(iv) We have detected a small solvent isotope effect for G-quartet aggregates. That is, the size of G-quartet aggregates is slightly larger in D<sub>2</sub>O than in H<sub>2</sub>O.

(v) While the added NaCl increases the population of G-quartet aggregates, the length of the 5'-GMP aggregates appears to be insensitive to the presence of NaCl in solution.

**Acknowledgment.** This work was supported by research grants from the Natural Sciences and Engineering Research Council (NSERC) of Canada, the Province of Ontario, and Queen's University. A.W. thanks the Province of Ontario for an Ontario Graduate Scholarship. R.I. thanks Queen's University for an R. S. McLaughlin Fellowship. We wish to thank an anonymous reviewer for very helpful comments.

JA042794D

(54) Wang, Y.; Patel, D. J. *J. Mol. Biol.* **1993**, *234*, 1171–1183.